THERMO-ECONOMIC COMPARISON OF ORGANIC RANKINE AND CO_2 CYCLE SYSTEMS FOR LOW-TO-MEDIUM TEMPERATURE APPLICATIONS

Xiaoya Li[1,2], Jian Song[2], Michael Simpson[2], Kai Wang[2],
Paul Sapin[2], Gequn Shu[1,*], Hua Tian[1], Christos N. Markides[2,+]

[1] State Key Laboratory of Engines (SKLE), Tianjin University, Tianjin, China
sgq@tju.edu.cn

[2] Clean Energy Processes (CEP) Laboratory, Imperial College London, London, United Kingdom
c.markides@imperial.ac.uk

*,+ Corresponding Author

ABSTRACT

Organic Rankine cycle (ORC) power systems are a well-established technology for low-to-medium temperature heat-conversion applications. Recently, CO_2-cycle power systems have emerged as another promising heat-to-power conversion technology and have been receiving increased interest due to certain advantages offered by the working fluid (e.g., non-flammable, high-temperature stability) and system compactness. However, it remains a challenge to select the appropriate technology between ORC and CO_2 power-cycle systems for different applications, as these can span a wide range of scales and heat-source conditions, particularly from an integrated thermodynamic and economic perspective. This paper presents a comprehensive thermo-economic comparison of ORC and CO_2 power systems with various architectures (i.e., with or without recuperation) in the specific context of power generation from two representative low- and medium-temperature heat sources, namely, brine in geothermal heat applications, and exhaust gases in waste-heat recovery from internal combustion engine applications. Expansion devices suitable for the given power scales, i.e., reciprocating-piston expanders and radial-inflow turbines, are considered and compared using comprehensive component-level models. Based on thermodynamic and economic performance analyses, technology selection maps for power generation from the pre-defined low- and medium-temperature heat sources are generated using the net power output and specific investment cost as key performance indicators. These performance selection maps allow for quick and effective decision making in choosing the optimal power cycles and system designs for geothermal exploitation, engine waste-heat recovery and other relevant heat-to-power applications.

1. INTRODUCTION

Of the alternatives to steam Rankine cycles (RC), organic Rankine cycle (ORC) systems are the most reliable and effective, and are already available on the market for a range of power scales. They offer the ability to exploit low-to-medium temperature heat sources in the field of both renewable energy, like geothermal, biomass and solar (Freeman *et al.*, 2017a, 2017b; Ramos *et al.*; 2018; Petrollese and Cocco, 2019), and industrial waste heat, such as combustion exhaust gases from cement plants, steel works and engines (Lecompte et al., 2017; Chatzopoulou *et al.*, 2017, 2019). Although organic working fluids bring high conversion efficiency and a reduction in the size of the system relative to a steam RC system, their unfavourable environmental and safety characteristics related to flammability and decomposition may hinder the adoption of ORC technology in the future, especially under the pressure from increasingly strict legislation (EPA, 2016). Recently, CO_2-cycle systems have started to gain significant interest from both industry and academia. The adoption of CO_2 as the working fluid enables more compact system design, lower investment costs, higher flexibility and lower environmental impact. Therefore, CO_2-cycle systems, normally appearing in the form of transcritical and supercritical CO_2-cycle systems, may become a strong competitor of ORC systems in low-to-medium heat recovery. An extensive overview by Omar *et al*. (2019) on three unconventional waste-heat recovery cycles focusing on eleven different applications demonstrated that CO_2 cycles with appropriate designs can be highly efficient for recovering low-to-medium temperature heat.

Li *et al*. (2014) conducted a comparative thermo-economic analysis of basic and recuperative CO_2-cycle and ORC systems for geothermal sources at 90-120 ℃; and found that the ORC system with R600a as the working fluid obtains the maximum net power. Similarly, Li *et al*. (2016) evaluated the thermodynamic performance of CO_2-cycle systems and R245fa-based ORC systems for 160 ℃ heat sources. The results proved the need for a recuperator to improve the thermal efficiency for both cycles, and also found that the ORC system outperforms the CO_2-cycle systems. Yet, another comparative investigation led by Klemencic *et al*. (2016) on RC, ORC and three CO_2-cycle systems for heat recovery from a cement plant showed that CO_2-cycle systems could offer better thermal efficiency and generate more net power than RC and ORC systems currently in service. Astolfi *et al*. (2018) compared four CO_2-cycle systems and four ORC systems for exploiting 30-MW_{th} heat sources with temperature of 200-600 ℃. Selection maps based on thermodynamic analysis highlighted that CO_2-cycle systems are preferable for heat sources above 300 ℃ while ORC systems are more competitive for lower temperature heat sources. Shu *et al*. (2016) optimized a CO_2-cycle system and R123 ORC system for gasoline engine waste-heat recovery: thermo-economic analysis indicated that the turbine size parameter in the CO_2-cycle systems was rather smaller than that in the ORC systems. Yoon *et al*. (2017) focused on the off-design performance comparison of an ORC system and a transcritical CO_2-cycle system for waste-heat recovery of a micro gas turbine. The findings led to ORC systems being proposed in the scenario operating at full load conditions while the CO_2-cycle systems were more suitable at low load conditions.

From the aforementioned research, CO_2-cycle systems have been studied and compared with the state-of-art ORC systems in various applications as an emerging technology for heat-to-power conversion. However, individual results targeted at specific heat sources and derived from various systems, operating parameters and working fluids make it difficult for cross-comparison between the two technologies. Moreover, most previous studies only focus on thermodynamic performance while economic performance comparison is ignored, although investment cost is also one of the most critical considerations for technology selection and implementation. The aim of the current work is to present comprehensive comparison and selection maps of ORC systems and CO_2-cycle systems from both thermodynamic and economic perspectives. Geothermal brine and exhaust gases from marine engines are selected as representatives of low-to-medium temperature heat sources to feed the ORC systems and CO_2-cycle systems, where both basic and recuperative architectures are considered. The paper also goes beyond the existing literature since expansion devices suitable for the given power scales, reciprocating-piston expanders and radial-inflow turbines, are considered and compared using comprehensive component-level models. Subcritical ORC systems adopting commercial HFC (R245fa), alkane representative (R600) and next generation refrigerant (R1233zd) working fluids are considered, as well as transcritical CO_2-cycle systems with and without recuperation are investigated.

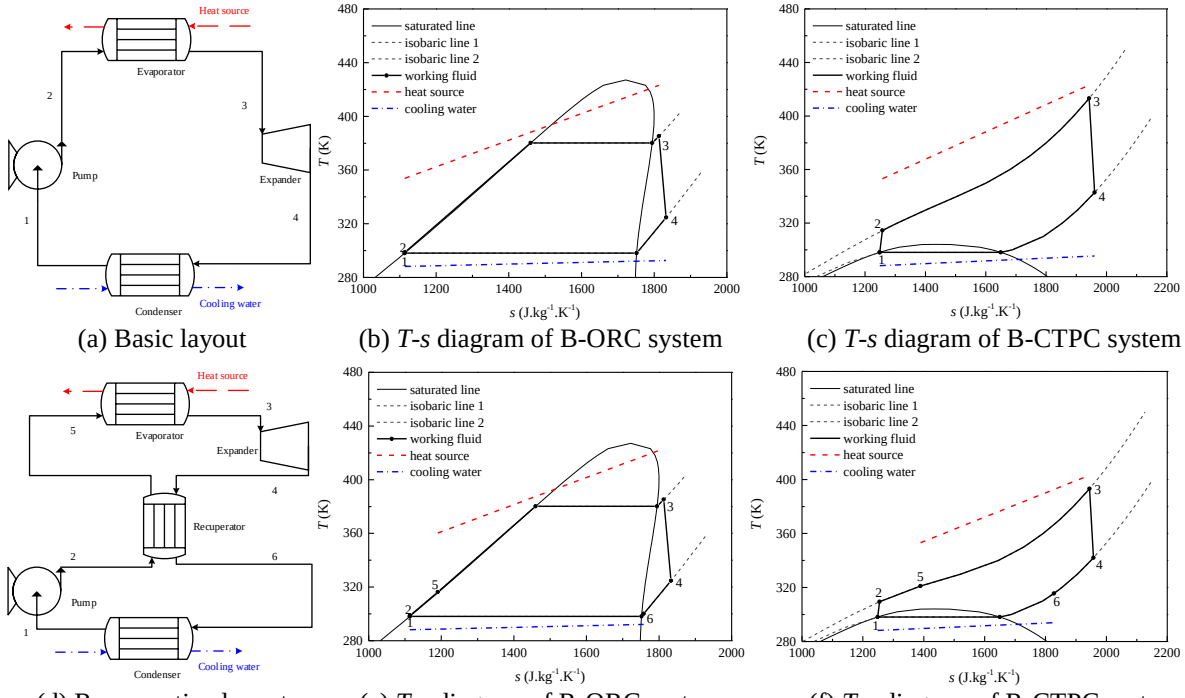
2. METHODOLOGY

2.1 System Description

Four systems, i.e., a basic ORC system (B-ORC), a recuperative ORC system (R-ORC), a basic CO_2 transcritical power cycle system (B-CTPC) and a recuperative CO_2 transcritical power cycle system (R-CTPC) are considered. The system schematics and the corresponding *T-s* diagrams are shown in Figure 1. The basic systems comprise a pump, an evaporator (or a gas heater), an expander and a condenser, while a recuperator is added in the recuperative systems.

Geothermal brine with temperatures of 100-200 ℃ and mass flowrates of 15-50 kg/s, and exhaust gases from marine engines with temperatures of 200-300 ℃ and mass flowrates of 20-120 kg/s are chosen as the representative heat sources. The minimum outlet temperature is set to be 80 ℃ for the brine (Hettiarachchi *et al*., 2007), and 160 ℃ for the exhaust gases (Yang and Yeh, 2015). The heat sink is considered to be cooling water at 15 ℃ for all systems and the condensation temperature set to 25 ℃. As concluded by van Kleef *et al.* (2019), the pinch point temperature constraints are not required when minimizing the costs while they are required for maximizing the power output, the pinch-point temperature differences in the heat exchangers are set as a conservative 6 ℃ for simplicity and as is common practice in such studies (Song *et al*., 2015, 2018). The pump isentropic efficiency is fixed at 0.8. For ORC systems, a superheat degree of 5 ℃ is applied to avoid liquid phase in the expander. A MATLAB code has been developed, incorporating detailed components models and economic models,

to perform the thermo-economic performance analysis of the selected systems. Fluid thermodynamic properties are obtained from NIST REFPROP database.



(a) Basic layout (b) *T-s* diagram of B-ORC system (c) *T-s* diagram of B-CTPC system

(d) Recuperative layout (e) *T-s* diagram of R-ORC system (f) *T-s* diagram of R-CTPC system

Figure 1: System schematic and corresponding *T-s* diagrams of the four systems considered in this study, i.e., the basic and recuperative ORC and CO_2 transcritical power cycles.

2.2 Heat Exchanger Models

Shell-and-tube heat exchangers are selected. The Bell-Delaware method (Kuppan, 2013) is used to calculate heat transfer coefficients (HTCs) and pressure drops.

The shell-side HTC, α_s, and pressure drop, ΔP_s, are given by:

$$\alpha_s = j_i \frac{c_{p,s} G_s}{\mathrm{Pr}_s^{2/3}} \left(\frac{\mu_s}{\mu_w} \right)^{0.14} j_c j_l j_b j_s j_r \tag{1}$$

$$\Delta P_s = \left[(N_b - 1) R_b R_l + 2 \left(1 + \frac{N_{tcw}}{N_{tcc}} \right) R_b R_s \right] \frac{2 f_s N_{tcc} G_s^2}{\rho_s} \left(\frac{\mu_s}{\mu_w} \right)^{-0.14} + \frac{(2 + 0.6 N_{tcw}) G_w^2}{2 \rho_s} N_b R_l \tag{2}$$

where j_i, j_c, j_l, j_b, j_s and j_r, are correction factors for the ideal HTC, baffle cut and spacing, baffle leakage effects, bundle bypass flow, variable baffle spacing in the inlet and outlet sections, and adverse temperature gradient buildup in laminar flow; c_p is the specific heat capacity; μ_s and μ_w are the viscosities at the bulk mean and wall temperatures; Pr is the Prandtl number; N_b, N_{tcc} and N_{tcw} are the number of baffles, the number of effective tube rows in crossflow, and the number of effective tube rows in baffle window; R_b, R_l and R_s are correction factors for bundle bypass effects, baffle leakage effects and unequal baffle spacing at inlet and outlet; f_s is the friction factor; G is a mass flow flux; and ρ is a density.

The tube-side HTC is calculated with the corresponding heat transfer correlation based on the working fluid and its phase. The HTCs for single phase flow, evaporation and condensation can be obtained from the Dittus-Boelter correlation, the Cooper nucleate pool-boiling correlation and the Dobson correlation (Kuppan, 2013), respectively. The HTCs of CO_2 are calculated by the Petukhov-Kirillov correlation for single phase, by the Petukhov-Krasnoshchekov-Protopopov correlation for supercritical phase and by the Chen correlation for condensation (Shu *et al.*, 2016). Detailed equations are omitted here for brevity. The tube-side pressure drop, ΔP_t, is given by:

$$\Delta P_t = \frac{1.5 G^2}{2\rho} + \frac{f_t L G^2 Z_t}{2 d_i \rho \varphi_t} + \frac{G^2}{2\rho} (K_c + K_e) Z_t + \frac{4 Z_t G^2}{2\rho} \tag{3}$$

where f_t is friction factor; L is tube length; d_i is tube inner diameter; Z_t is the number of passes; K_c and K_e are the contraction and expansion loss coefficients; and φ_t is a parameter related to the ratio of viscosity at bulk mean temperature and wall temperature.

2.3 Expander Models

The radial-inflow turbine is modelled by a 1-D mean-line method. MATLAB function *fmincon* is chosen as the solver to maximise the turbine efficiency (by minimising the negative of the efficiency), under nonlinear constraints considering the limitations of the turbine geometric parameters and manufacturing capabilities in practical applications. Several key parameters are chosen as decision variables, i.e., the nozzle velocity coefficient, φ; the rotor velocity coefficient, ψ; the velocity ratio, $\bar{u}_1$; the reaction degree, Ω; the wheel diameter ratio, $\bar{D}_2$; the absolute flow angle at rotor inlet, α_1; and the relative flow angle at rotor outlet, β_2. The turbine efficiency, η_T, can be expressed as:

$$\eta_T = \eta_u - \zeta_f - \zeta_l \tag{4}$$

$$\eta_u = 2\bar{u}_1 \cdot \left(\varphi \cdot \sqrt{1-\Omega} \cdot \cos\alpha_1 - \bar{D}_2^2 \cdot \bar{u}_1 + \bar{D}_2 \cdot \psi \cdot \cos\beta_2 \cdot \left[\Omega + \varphi^2 \cdot (1-\Omega) - 2\varphi \cdot \sqrt{1-\Omega} \cdot \bar{u}_1 \cos\alpha_1 + \bar{D}_2^2 \cdot \bar{u}_1^2 \right]^{1/2} \right) \tag{5}$$

$$\zeta_f = \frac{f}{1.36\times10^6} \cdot \frac{u_1^3}{\dot{m} \cdot \Delta h_s} \cdot \frac{D_1^2}{v_1} \tag{6}$$

$$\zeta_l = \begin{cases} 1.3 \cdot \dfrac{\delta}{l_m} \cdot (\eta_u - \zeta_f), & \dfrac{\delta}{l_m} \le 0.05 \\ \left(0.05 + 0.31 \cdot \dfrac{\delta}{l_m} \right) \cdot (\eta_u - \zeta_f), & \dfrac{\delta}{l_m} > 0.05 \end{cases} \tag{7}$$

where η_u is the peripheral efficiency; ζ_f is the friction loss; ζ_l the leakage loss; f the friction loss factor; $\dot{m}$ the mass flowrate; u_1 the fluid velocity at rotor inlet; Δh_s the isentropic entropy drop; v_1 the specific volume at rotor inlet; δ the tip clearance; and l_m the average rotor blade height.

Regarding the reciprocating-piston expander, the steady-state performance is predicted using a dynamic lumped-mass model. Optimized maps for each working fluid are generated by capturing the major loss mechanisms, including the in-cylinder losses (i.e., the gas-to-wall instantaneous heat transfer and the mass leakage past the piston rings), the pressure losses (due to the working-fluid flow through the area restrictions of the intake and exhaust valves) and the direct mechanical power losses (due to friction between the various moving parts). The overall isentropic efficiency, η_{is}, is defined as:

$$\eta_{is} = \frac{\dot{W}_{exp}}{\dot{m}(h_{in} - h_{out})} \tag{8}$$

$$\frac{dm}{dt} = \dot{m}_{in} - \dot{m}_{out} \tag{9}$$

$$\frac{d}{dt}(mh) = \dot{Q} + V\frac{dP}{dt} + \sum \dot{m}_{in} h_{in} - \sum \dot{m}_{out} h_{out} \tag{10}$$

where W_{exp} denotes the expansion power; h the specific enthalpy; $\dot{Q}$ the heat load; V the cylinder volume; and P the pressure. Subscripts 'in' and 'out' refer to inlet and outlet, respectively.

2.4 Economic Models

The specific investment cost, *SIC*, the ratio of the system cost to the net power output, is chosen to evaluate the system economic performance. Each main component is costed by the module costing technique to obtain the bare module cost, C_{BM}, which is further modified by the chemical engineering plant cost index (CEPCI) to obtain the cost. All component costs are summed to get the capital cost of the systems. Equations are omitted here and can be found in Shu *et al.*, 2016.

3. RESULTS

3.1 Geothermal Application

Thermo-economic analyses are performed for geothermal exploitation and the optimized performance

maps with different expanders are depicted in Figure 2 and Figure 3, with the working fluids corresponding to the optimal performance labelled. Figure 2(a) shows that the R-ORC system outperforms the other three systems from the perspective of net power production when a radial-inflow turbine is used for the given heat-source range, because the flowrate of the working fluid in R-ORC systems is slightly higher than in B-ORC systems, while pumping power consumption degrades the net power output in CTPC systems. Although the optimal working fluid varies with the heat-source temperature, the differences are not that remarkable. The critical temperatures of R245fa (427.2 K), R600 (425.1 K) and R1233zd (438.8 K) are quite similar. Hence, the maximum power that can be achieved with said fluids at similar evaporation temperatures, determined by the pinch point. Furthermore, the radial-inflow turbine can achieve isentropic efficiencies of around 0.84 after optimization, for each working fluid. Figure 2(b) indicates that the B-ORC system is the most cost-effective technology thanks to the simple architecture which can yield comparable net power output with the R-ORC systems without the need for additional heat exchangers introduced.

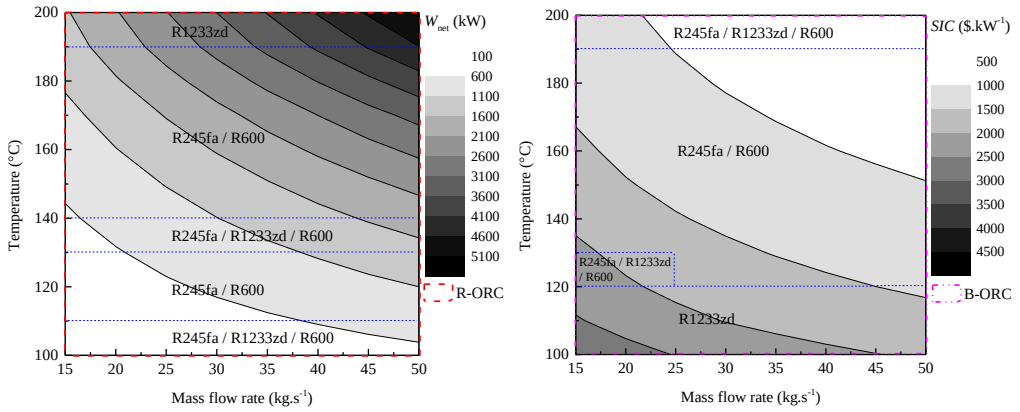


Figure 2: Optimized performance maps with radial-inflow turbine based on: (a) net power output, and (b) *SIC* for geothermal exploitation.

With reciprocating-piston expanders, the R-ORC system continues to perform most strongly over much of the given heat-source range, as shown in Figure 3(a). However, at higher heat-source temperature, the R-CTPC system provides the maximum net power output, as the transcritical heating process of CO_2 introduces a better thermal match with the heat source and thus CO_2 can be heated to a higher temperature, which further benefits the recuperative process. It is noteworthy that the R-CTPC system competes with the R-ORC system at heat-source temperatures of 140-150 ℃, which is mainly caused by the non-monotonic isentropic efficiency variation of the piston expander with different inlet temperatures and pressures. Figure 3(b) also shows that the B-ORC system has the lowest *SIC*, with R600 as the best working fluid because of the low heat transfer areas required.

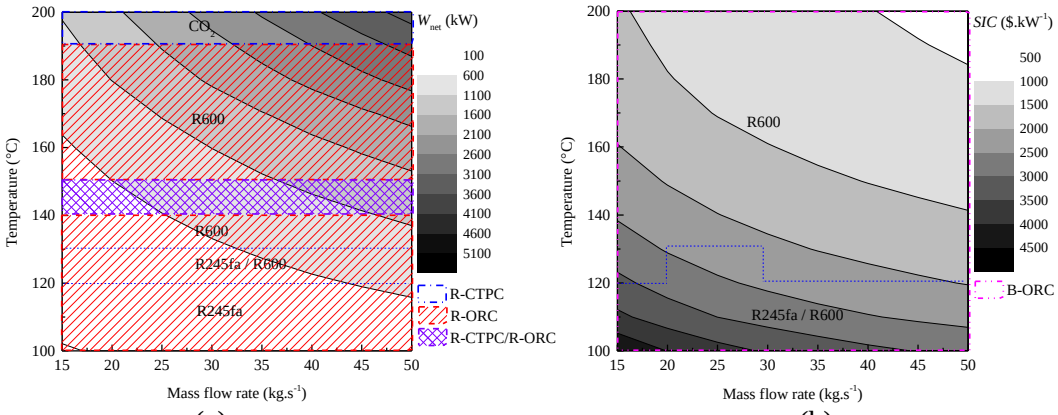


Figure 3: Optimized performance maps with reciprocating-piston expander based on: (a) net power output, and (b) *SIC* for geothermal exploitation.

3.2 Marine Engine Waste-heat Recovery

With radial-inflow turbines (Figure 4), the R-ORC system with R1233zd as the working fluid can generate the maximum power if the temperature of the exhaust gases is lower than 230 ℃, while the R-CTPC system is the best option from the thermodynamic perspective when the heat-source temperature is higher. The recuperator significantly improves the net power output by 23-62% in the CTPC systems when the heat-source temperature increases from 200 to 300 ℃, while it is only increased by 10-17% in the ORC systems with the three working fluids. However, the pump cost in the CTPC system is much higher than that in the ORC system; hence the B-ORC system obtains the minimum *SIC*.

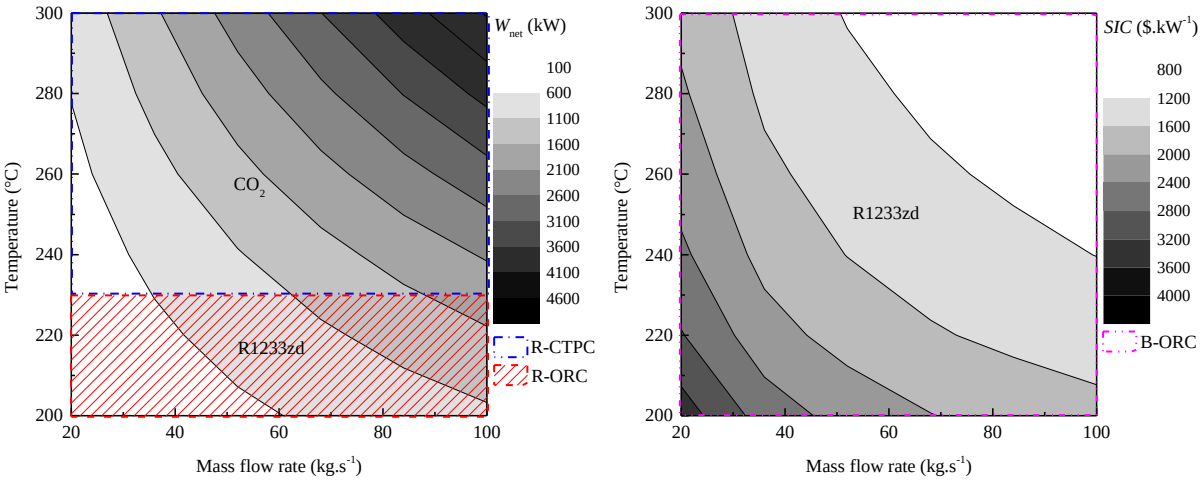


Figure 4: Optimized performance maps with radial-inflow turbine based on: (a) net power output, and (b) *SIC* for marine engines waste-heat recovery.

With reciprocating-piston expanders, the R-CTPC system is the most attractive architecture in terms of the net power output, as shown in Figure 5(a). Apart from the better thermal match with the heat source, the isentropic efficiencies of the expander in the CTPC systems are also higher than those in the ORC systems at higher expander inlet temperatures and pressures. With higher inlet pressure, i.e., higher evaporation temperature in the ORC systems, the isentropic efficiency of the expander decreases from 0.80 to 0.54 for R245fa, from 0.75 to 0.66 for R600 and from 0.65 to 0.45 for R1233zd. The piston expander can maintain a considerable isentropic efficiency of around 0.80 when its inlet temperature is above 200 ℃. Although the B-ORC system is still the most cost-effective technology, R600 appears as the optimal working fluid with the reciprocating-piston expander (see Figure 5(b)), which is quite different from that with radial-inflow turbine (see Figure 4(b)). The piston expander is found to exhibit a weaker performance with R1233zd than with the other two working fluids.

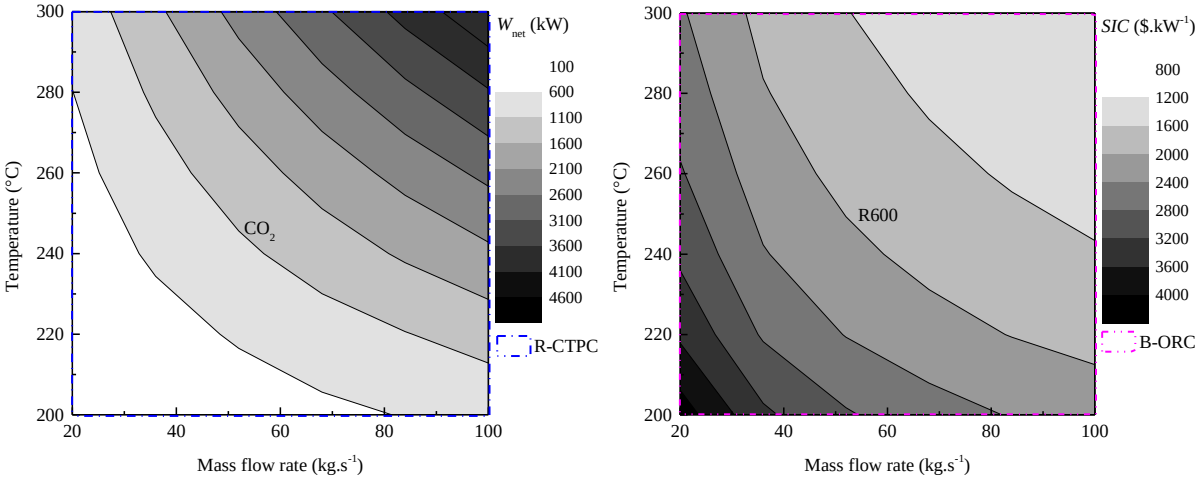
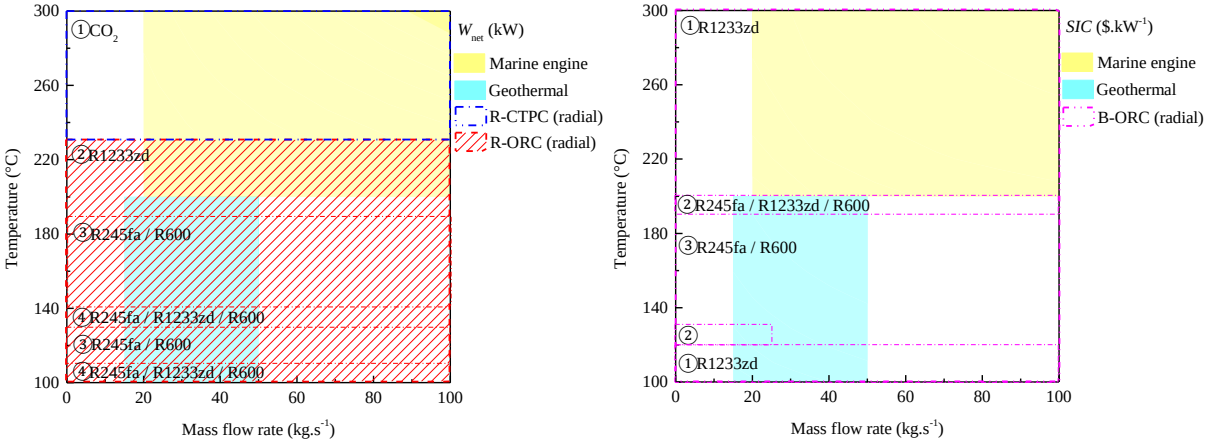


Figure 5: Optimized performance maps with reciprocating-piston expander based on: (a) net power output, and (b) *SIC* for marine engines waste heat recovery.

3.3 Generalized Selection Maps

As reflected by the performance maps presented in the previous section, the optimal working fluid is much more sensitive to the heat-source temperature than to the mass flowrate, with the same working fluid favoured across different heat-source mass flowrates. Therefore, we extended the maps for generalized heat sources with temperatures of 100-300 ℃ and mass flowrates of 0-100 kg/s. The selection maps of both the net power output and the *SIC* are given in Figure 6 with the geothermal and marine engine applications coloured in the corresponding areas.

It can be concluded that a recuperator is preferable for maximum power production, although it would increase the costs. CO_2 systems can generate more net power at higher heat-source temperatures, while the organic working fluids are better at lower heat-source temperatures. The B-ORC system appears as the best option among these four systems in terms of *SIC*. Moreover, the radial-inflow turbine outperforms the reciprocating-piston expander since it can achieve higher isentropic efficiencies.



(a) (b)

Figure 6: Selection maps based on: (a) net power output, and (b) *SIC* for power conversion from low-to-medium temperature heat sources.

4. CONCLUSIONS

A comparison of ORC and CO_2 power systems has been performed for heat-to-power conversion applications. Geothermal heat and waste-heat recovery from marine engine exhaust gases are selected as heat sources, and exploited with basic and recuperative ORC and CO_2 systems employing two suitable expanders, i.e., radial-inflow turbines and reciprocating-piston expanders. Thermodynamic and economic performance selection maps are generated, from which the following conclusions are drawn:

- A recuperator is favoured for high power outputs, while basic systems without a recuperator are more economically viable. The R-CTPC system outperforms the other systems at high heat-source temperatures (i.e., above 230 ℃ indicated in the present study), while the R-ORC system is much more suitable at lower heat-source temperatures in terms of net power output.
- Radial-inflow turbines are more attractive than the reciprocating-piston expanders for both CO_2 and organic working fluids for the given heat-source and power-output ranges, i.e., for plants from 100s of kW up to the order of MW. Future work can focus at smaller scales, i.e., 10s of kW and up to a few 100 kW, where piston expanders are extended to be more suitable.
- The optimal working fluid in ORC systems is much more sensitive to the heat-source temperature than to the heat-source mass flowrate, hence the selection of the working fluids can be conducted according to the heat-source temperature.

REFERENCES

Astolfi, M., Alfani, D., Lasala, S., Macchi, E., 2018, Comparison between ORC and CO_2 power systems for the exploitation of low-medium temperature heat sources, *Energy*, vol. 161, p. 1250-61.

Chatzopoulou, M. A., Markides, C. N., 2017, Thermodynamic optimisation of a high-electrical efficiency integrated internal combustion engine–organic Rankine cycle combined heat and power system, *Appl. Energy*, vol. 226, p. 1229-51.

Chatzopoulou, M. A., Simpson, M., Sapin, P., Markides, C. N., 2019, Off-design optimisation of organic Rankine cycle (ORC) engines with piston expanders for medium-scale combined heat and power applications, *Appl. Energy*, vol. 238, p. 1211-36.

EPA, 2016, Rules and Regulations, *Federal Register*, vol. 81, no. 231: p. 86778-895.

Freeman, J., Hellgardt, K., Markides, C. N., 2017, Working fluid selection and electrical performance optimisation of a domestic solar-ORC combined heat and power system for year-round operation in the UK, *Appl. Energy*, vol. 186, p. 291-303.

Freeman, J., Guarracino, I., Kalogirou, S.A., Markides, C. N., 2017, A small-scale solar organic Rankine cycle combined heat and power system with integrated thermal energy storage, *Appl Therm Eng*, vol. 127, p. 1543-54.

Hettiarachchi, H., Golubovic, M., Worek, W., Ikegami, Y., 2007, Optimum design criteria for an organic Rankine cycle using low-temperature geothermal heat sources, *Energy*, vol. 32, p. 1698-706.

Klemencic, G., Flegkas, S., Werner, A., Haider, M., Leibinger, H., 2016, Comparison of conventional and CO_2 power generation cycles for waste heat recovery, *The 5th International Symposium – Supercritical CO_2 Power Cycles*, p. 1-15.

Kuppan, T., 2013, *Heat Exchanger Design Handbook, Second Edition*, CRC Press.

Lecompte, S., Oyewunmi, O. A., Markides, C. N., Lazova, M., Kaya, A., *et al*., 2017, Case study of an organic Rankine cycle (ORC) for waste heat recovery from an electric arc furnace (EAF), Energies vol. 10, p. 649.

Li, M., Wang, J., Li, S., Wang, X., He, W., Dai, Y., 2014, Thermo-economic analysis and comparison of a CO_2 transcritical power cycle and an organic Rankine cycle, *Geothermics*, vol. 50, p. 101-11.

Li, L., Ge, Y., Luo, X., Tassou, S., 2016, Thermodynamic analysis and comparison between CO_2 transcritical power cycles and R245fa organic Rankine cycles for low grade heat to power energy conversion, *Appl Therm Eng*, vol. 106, p. 1290-9.

Omar, A., Saghafifar, M., Mohammadi, K., Alashkar, A., Gadalla, M., 2019, A review of unconventional bottoming cycles for waste heat recovery: Part II – Applications, *Energy Convers Manag*, vol. 180, p. 559-83.

Petrollese, M., Cocco, D., 2019, Robust optimization of the preliminary design of solar organic Rankine cycle (ORC) systems, *Energy Convers Manag*, vol. 184, p. 338-49.

Ramos, A., Chatzopoulou, M. A., Freeman, J., Markides, C. N., 2018, Optimisation of a high-efficiency solar-driven organic Rankine cycle for applications in the built environment, *Appl Energy*, vol. 228, p. 755-65.

Shu, G., Shi, L., Tian, H., Li, X., Huang, G., Chang, L., 2016, An improved CO_2-based transcritical Rankine cycle (CTRC) used for engine waste heat recovery, *Appl Energy*, vol. 176, p. 171-82.

Song J., Li X., Ren X., Gu C., 2015, Parametric analysis of a dual loop Organic Rankine Cycle (ORC) system for engine waste heat recovery, *Energy Convers Manag*, vol. 105, p. 995-1005.

Song J., Li X., Ren X., Gu C., 2018, Performance improvement of a preheating supercritical CO_2 (S-CO_2) cycle based system for engine waste heat recovery, *Energy Convers Manag*, vol. 161, p. 225-33.

van Kleef L.M.T., Oyewunmi, O. A., Markides, C. N., Multi-objective thermo-economic optimization of organic Rankine cycle (ORC) power systems in waste-heat recovery applications using computer-aided molecular design techniques, *Appl Energy*, vol. 251, p. 112513.

Yang, M., Yeh, R., 2015, Thermo-economic optimization of an organic Rankine cycle system for large marine Diesel engine waste heat recovery, *Energy*, vol. 82, p. 256-68.

Yoon, S., Kim, M., Kim, I., Kim, T., 2017, Comparison of micro gas turbine heat recovery systems using ORC and trans-critical CO_2 cycle focusing on off-design performance, *Energy Procedia*, vol. 129, p. 987-94.

ACKNOWLEDGEMENT

This work was supported by the National Key R&D Program of China (2018YFB01059000) and the UK Engineering and Physical Sciences Research Council (EPSRC) [grant number EP/P004709/1]. The authors would also like to thank China Scholarship Council for a joint-PhD scholarship that supported XL during this research. Data supporting this publication can be obtained on request from cep-lab@imperial.ac.uk.